

# A Young Brown Dwarf Companion to DH Tauri<sup>1</sup>

Yoichi Itoh<sup>2</sup>, Masahiko Hayashi<sup>3</sup>, Motohide Tamura<sup>4</sup>, Takashi Tsuji<sup>5</sup>, Yumiko Oasa<sup>2</sup>, Misato Fukagawa<sup>6</sup>, Saeko S. Hayashi<sup>3</sup>, Takahiro Naoi<sup>6</sup>, Miki Ishii<sup>3</sup>, Satoshi Mayama<sup>7</sup>, Jun-ichi Morino<sup>3</sup>, Takuya Yamashita<sup>3</sup>, Tae-Soo Pyo<sup>3</sup>, Takayuki Nishikawa<sup>8</sup>, Tomonori Usuda<sup>3</sup>, Koji Murakawa<sup>3</sup>, Hiroshi Suto<sup>3</sup>, Shin Oya<sup>3</sup>, Naruhisa Takato<sup>3</sup>, Hiroyasu Ando<sup>4</sup>, Shoken M. Miyama<sup>4</sup>, Naoto Kobayashi<sup>5</sup>, and Norio Kaifu<sup>4</sup>,

## ABSTRACT

We present the detection of a young brown dwarf companion DH Tau B associated with the classical T Tauri star DH Tau. Near-infrared coronagraphic observations with CIAO on the Subaru Telescope have revealed DH Tau B with  $H = 15$  mag located at  $2''.3$  (330 AU) away from the primary DH Tau A. Comparing its position with a *Hubble Space Telescope* archive image, we confirmed that DH Tau A and B share the common proper motion, suggesting that they are physically associated with each other. The near-infrared color of DH Tau B is consistent with those of young stellar objects. The near-infrared spectra of DH Tau B show deep water absorption bands, a strong K I absorption line, and a moderate Na I absorption line. We derived its effective temperature and surface gravity of  $T_{\text{eff}} = 2700 - 2800$  K and  $\log g = 4.0 - 4.5$ , respectively, by comparing the observed spectra with synthesized spectra of low-mass objects. The location of DH Tau B on the HR diagram gives its mass of  $30 - 50 M_{\text{Jupiter}}$ .

*Subject headings:* stars: individual (DH Tau) — stars: pre-main sequence — stars: low-mass, brown dwarfs — techniques: high angular resolution

---

<sup>2</sup>Graduate School of Science and Technology, Kobe University, 1-1 Rokkodai, Nada, Kobe, Hyogo 657-8501, Japan, yitoh@kobe-u.ac.jp

<sup>3</sup>Subaru Telescope, 650 N'Aohoku Pl., Hilo, Hawaii 96720, USA

<sup>4</sup>National Astronomical Observatory, 2-21-1 Osawa, Mitaka, Tokyo 181-8588, Japan

<sup>5</sup>Institute of Astronomy, The University of Tokyo, 2-21-1 Osawa, Mitaka, Tokyo 181-8588, Japan

<sup>6</sup>Graduate School of Science, The University of Tokyo, 2-21-1 Osawa, Mitaka, Tokyo 181-8588, Japan

<sup>7</sup>Graduate School of Science and Engineering, Waseda University, 3-4-1 Okubo, Shinjuku, Tokyo 169-8555, Japan

<sup>8</sup>Department of Astronomical Science, Graduate University for Advanced Studies (Sokendai), 650 N. A'ohoku Place, Hilo, Hawaii 96720, USA

<sup>1</sup>Based on data collected at the Subaru Telescope, which is operated by the National Astronomical Observatory of Japan.

## 1. INTRODUCTION

Brown dwarfs are objects with their masses less than  $0.08 M_{\odot}$ . Unable to sustain stable hydrogen burning in their cores, they contract monotonously as they release gravitational energy into radiation. Their luminosities are small; even a  $0.07 M_{\odot}$  brown dwarf has a luminosity of only  $10^{-4} L_{\odot}$  at its age of  $10^9$  yr (Burrows et al. 1997; Baraffe et al. 2003). Their faintness has prevented their discovery despite an early prediction of their existence (Hayashi & Nakano 1963). Since G1229B was first identified as a bona fide brown dwarf (Nakajima et al. 1995; Oppenheimer et al. 1995), more than 300 brown dwarfs have been discovered by photometric and spectroscopic observations including Doppler shift measurements. While more than half of stars are found in binary systems, only  $\sim 20$  brown dwarfs out of 300 have so far been identified as companions to stars.

The deficiency of companion brown dwarfs led some researchers to favor gravitational collapse of molecular cloud cores as their formation mechanism, similar to that of stars (Bonnell & Bastien 1992; Bate 2000). It has, on the other hand, also been proposed that brown dwarfs may form from circumstellar disks as companions to stars (Rice et al. 2003), similar to the possible mechanism of giant planet formation initiated by gravitational instability of a disk. Successive dynamical evolution of such a star and brown dwarf system with other stars in a newly formed cluster may eject the brown dwarf from the system (Reipurth & Clarke 2001). It is thus important to find young brown dwarf companions to study their formation mechanism.

Although young brown dwarfs are mostly found in star forming regions located far away when compared with nearby stars, they are bright and relatively easy to be detected; a  $0.03 M_{\odot}$  brown dwarf is  $10^{-2} L_{\odot}$  at its age of  $10^6$  yr (Burrows et al. 1997; Baraffe et al. 2003). Near-infrared imaging with high sensitivity indeed detected many young brown dwarfs in star forming regions (e.g. Oasa et al. 1999; Zapatero-Osorio et al. 2002; Allen et al. 2002; Mainzer & McLean 2003; Luhman et al. 2003). Only a small number of brown dwarf companions, however, has so far been found around young stars (CoD–33°7795 B, Lowrance et al. 1999; GG Tau Bb, White et al. 1999; HR 7329 B, Lowrance et al. 2000), as is similar to the case of companions to main sequence stars. Very recently, Chauvin et al. (2004) announced the discovery of a planetary-mass companion candidate to a young brown dwarf.

In this article we report the detection of a faint brown dwarf companion to DH Tau with CIAO (Coronagraphic Imager with Adaptive Optics; Tamura et al. 2000) mounted on the Subaru Telescope. DH Tau is a classical T Tauri star associated with the Taurus molecular cloud and has a visual extinction of 0.0–1.5 mag (Strom et al. 1989; White & Ghez 2001). It has a mass and age of  $0.25\text{--}0.5 M_{\odot}$  and  $10^5\text{--}4 \times 10^6$  yr, respectively (Hartigan et al. 1994; White & Ghez 2001), where the uncertainties arise mainly from that of bolometric luminosity. The companion is located 330 AU from the primary and has the effective temperature, mass and age of 2700 – 2800 K,  $0.03 - 0.05 M_{\odot}$  and  $3 \times 10^6 - 10^7$  yr, respectively.

We are conducting a near-infrared coronagraphic survey for proto-planetary disks and faint

companions around T Tauri stars. DH Tau was initially selected as a target for a proto-planetary disk. Its polarization angle is perpendicular to the nearby magnetic field direction, implying the existence of a circumstellar disk (Tamura & Sato 1989). Other target samples consist mainly of objects with circumstellar disks detected in the millimeter wavelengths (Kitamura et al. 2003). By near-infrared coronagraphic observations, a dozen of faint point sources are detected in the vicinity of the T Tauri stars. However, it is not yet confirmed by spectroscopic observations and proper motion measurements whether the faint sources are associated with the T Tauri stars or are background objects. The nature of these faint sources will be investigated in the future.

## 2. OBSERVATIONS AND DATA REDUCTION

The coronagraphic observations were carried out at  $H$ -band on 2002 November 23 and at  $J$ ,  $H$  and  $K$ -bands on 2004 January 8 with CIAO, which was equipped with a  $1024 \times 1024$  InSb Alladin II detector with a spatial scale of  $0''.0213 \text{ pixel}^{-1}$ . The spatial resolution provided by the adaptive optics system was  $0''.1$  (FWHM) under the natural seeing of  $\sim 0''.5$ . An occulting mask made of chrome on a sapphire substrate had a diameter of  $0''.6$ , within which the transmittance was a few tenths of a percent. This allowed us to measure the accurate position of the central object. We used a traditional circular Lyot stop with its diameter 80 % of the pupil.

For taking images at each band, we adjusted the telescope pointing finely so that the DH Tau primary (hereafter called DH Tau A) was placed at the center of the occulting mask. Three exposures of 10 sec each were coadded into one frame. After 6 frames of observations, both the telescope and the occulting mask were dithered by  $\sim 1''$ . DH Tau A was again placed at the center of the occulting mask, then additional 18 frames were taken. The total exposure time is 720 sec in each band. We observed SAO 76560 immediately after DH Tau as a reference star of the point spread function (PSF) under the same configuration. We also observed FS 111 for photometric calibration. Dark frames and dome flats with incandescent lamps were taken at the end of the night.

The Image Reduction and Analysis Facility (IRAF) was used for data reduction. A dark frame was subtracted from each object frame, then each object frame was divided by the dome-flat. Hot and bad pixels were removed from the frame. The peak position of the PSF moved slightly on the detector during the observations. This was caused by the difference in the atmospheric distortion between the infrared wavelength at which the images were taken and the optical wavelength at which the wavefront was sensed. We measured the peak positions of reference star PSF images with the RADPROFILE task and shifted them to have the same peak position. Since the Subaru Telescope is an alt-azimuth telescope and we used an instrument rotator, the position angle of the spider pattern changed with time. The reference star frames were hence rotated so that the position angle of the spider matched that of each object frame, and then combined. The combined reference star PSF was shifted so that its peak position coincided with the DH Tau A peak, which had been measured with the RADPROFILE task in each frame. The reference star PSF was then

renormalized so that its wing intensity level became the same as that of DH Tau A at  $\sim 1''$  away from its peak. The halo of DH Tau A was suppressed in each frame after the reference star PSF was subtracted, which allowed us to detect an object (hereafter called DH Tau B) that was located at  $2''34$  southeast of DH Tau A and was  $\sim 6$  mag fainter. Finally, all the 24 object frames were combined into one image.

The  $K$ -band spectroscopy of DH Tau B was made on 2003 November 8 with CISCO mounted on the Subaru Telescope. We used a grism with a spectral resolution of  $R (= \lambda/\Delta\lambda) \sim 440$  at  $2.2 \mu\text{m}$  and a slit width of  $0''.5$  under the typical seeing of  $0''.5$ . The adaptive optics system was not available for CISCO. In order to minimize the contamination of light from DH Tau A, we placed the slit on DH Tau B to be perpendicular to the line connecting DH Tau A and B. Using the  $K$ -band images taken just before the spectroscopic observations, we estimate that contaminated flux from the primary in the spectra is  $\sim 10\%$  of the flux of the secondary. DH Tau B was observed at 2 slit positions with a  $10''$  dithering to obtain sky data simultaneously. Two exposures of 300 sec each were made at each slit position. SAO 76860 (A0V) was used as a standard star for spectral calibration. The  $JH$ -band spectra were observed in the similar manner on 2004 January 9 with  $R \sim 300$  and the total integration time of 60 min.

We used IRAF for spectral data reduction again. Each dithered pair of object frames were subtracted from each other and divided by a flat field frame. We then geometrically transformed the frames to remove the curvature of the slit image caused by the grating. Wavelengths were calibrated using the OH lines in the sky portion of the spectrum with the uncertainty of  $10 \text{ \AA}$  rms. Individual spectra were extracted from the transformed images using the APALL task. The areas of the spectral images where the intensity of DH Tau B was more than 20% of its peak intensity at each wavelength were summed into an one-dimensional spectrum. The spectrum was then normalized and combined to produce the final spectrum. After the hydrogen absorption lines in the standard star spectrum were interpolated and removed, the object spectrum was divided by the standard star spectrum and was multiplied by a blackbody spectrum representing the standard star. The  $JH$ - and  $K$ -band spectra were scaled to the photometric magnitudes.

### 3. RESULTS AND DISCUSSION

#### 3.1. A Physical Companion

The  $K$ -band coronagraphic image of DH Tau is presented in Figure 1. DH Tau A, occulted by the mask, is located at the center, where the bright speckles are the residual halo of PSF subtraction. We do not detect any diffuse circumstellar structure. While near- and mid-infrared excesses and millimeter flux, possibly from a circumstellar structure are reported (Meyer et al. 1997a; Dutrey et al. 1996), any spatial-resolved image of the circumstellar structure has not been presented. Even with the coronagraph, we do not expect any detection of a circumstellar structure with such a short integration time, unless it is highly-flared (Itoh et al. 1998).

A point source (DH Tau B) was detected at the southeast of DH Tau A. We consider from the following arguments that DH Tau B is most likely a physical companion to DH Tau A. The offset of DH Tau B with respect to A was  $(\Delta\alpha, \Delta\delta) = (+1''.512 \pm 0''.003, -1''.791 \pm 0''.003)$  on 2004 January 8, corresponding to the angular separation and position angle of  $2''.344 \pm 0''.003$  ( $328.2 \pm 0.4$  AU) and  $139^\circ.83 \pm 0^\circ.06$ , respectively. These were  $2''.340 \pm 0''.006$  and  $139^\circ.56 \pm 0^\circ.17$ , respectively, on 2002 November 23 ( $(\Delta\alpha, \Delta\delta) = (+1''.518 \pm 0''.008, -1''.781 \pm 0''.008)$ ). The uncertainties are the standard deviation of the measurements of positions in each frame ( $0.008''$  and  $0.002''$  both in the  $\alpha$  and  $\delta$  directions, for the 2002 and 2004 observations respectively), and the uncertainties in the pixel scale and in the orientation of the detector<sup>2</sup>. Since any other object is not found in the small field of view of CIAO, and DH Tau B has not been recorded in any published catalog, the offsets of DH Tau B are derived only with the positions of DH Tau A and B.

DH Tau B was also detected in the *Hubble Space Telescope* archive data imaged on 1999 January 17 with the offset of  $(\Delta\alpha = +1''.531 \pm 0''.003, \Delta\delta = -1''.784 \pm 0''.003)$  or the separation and position angle of  $2''.351 \pm 0''.001$  and  $\theta = 139^\circ.36 \pm 0^\circ.10$ , respectively (Holtzman et al. 1995 for the pixel scale). The three measurements give consistent offsets within  $0''.02$ , comparable to the pixel size of CIAO, in both  $\alpha$  and  $\delta$  directions, suggesting that DH Tau A and B share a common proper motion in five years. Because DH Tau A has a proper motion of  $\delta_\alpha \sim +12 \pm 4$  mas/yr and  $\delta_\delta \sim -25 \pm 3$  mas/yr (Monet et al. 2003; Hanson et al. 2003; Zacharias et al. 2003) that could be easily detected against a background or foreground star with CIAO in five years of interval, DH Tau B should not be a background or foreground star. In fact, DH Tau B would have moved by  $(-0''.060, 0''.125)$  in five years if it had been a background star (see Figure 2).

DH Tau B is hence associated with the Taurus molecular cloud, where new born stars share a similar proper motion of  $\delta_\alpha \sim +6 \pm 7$  mas/yr and  $\delta_\delta \sim -22 \pm 6$  mas/yr (Jones & Herbig 1979). Two physically unrelated stars associated with the Taurus molecular cloud have a large chance to have similar proper motions that we cannot discern in five years. There is, however, a very small chance that an object with  $J = 15$  happens to be located within  $2''.3$  from DH Tau A. We expect 20 such objects in 1 arcdegree square, by extrapolating the luminosity function of low-mass objects associated with the Taurus molecular cloud (Itoh et al. 1996). If such objects are randomly distributed, chance probability that an isolated object is located at  $2''.3$  from DH Tau A is estimated as small as  $10^{-5}$ . We therefore conclude that DH Tau B is most likely a physical companion to DH Tau A.

---

<sup>2</sup>The pixel scale and the orientation of the detector were determined by observations of the Trapezium cluster (Simon et al. 1999). The pixel scale for the 2002 observations is  $0.02125 \pm 0.00003''$  pixel<sup>-1</sup>. Note that the pixel scale in Itoh et al. (2002) is misprinted. The detector of CIAO was replaced in 2003 Nov. The pixel scale for the new detector is  $0.02133 \pm 0.00002''$  pixel<sup>-1</sup>.

### 3.2. The Near-Infrared Spectrum

Photometry of DH Tau B gives its near-infrared magnitudes of  $15.71 \pm 0.05$ ,  $14.96 \pm 0.04$  and  $14.19 \pm 0.02$  at the  $J$ -,  $H$ - and  $K$ -bands, respectively. Its colors, together with those of DH Tau A, are plotted on the two color diagram in Figure 3. Both DH Tau A and B have the colors consistent with T Tauri stars. Note that the redder color of DH Tau B than DH Tau A does not explicitly indicate larger infrared excess of DH Tau B than DH Tau A. Because DH Tau B has a lower effective temperature as derived below (2700 K – 2800 K), than DH Tau A (3580 K; Hartigan et al. 1994), photospheric color of DH Tau B is expected to be redder than that of DH Tau A. Assuming DH Tau A and B have the same photospheric colors as early- and late-M dwarfs, respectively, infrared excesses of both objects are comparable.

The near-infrared spectra of DH Tau B are shown in Figure 4, where prominent water absorption bands are seen around  $1.4 \mu\text{m}$  and  $1.9 \mu\text{m}$ . These absorption bands are also prominent in the  $H$ -band spectrum of the giant planet candidate around a young brown dwarf (Chauvin et al. 2004). The absorption lines of K I and Na I were detected at  $1.25 \mu\text{m}$  and  $2.21 \mu\text{m}$ , respectively. Their equivalent widths are measured to be  $6.8 \pm 2.8 \text{\AA}$  and  $1.8 \pm 1.4 \text{\AA}$  for the K I and Na I lines, respectively, using the spectro-photometric bands defined by Gorlova et al. (2003). These characteristics suggest a low temperature of DH Tau B.

We compare the observed spectra with model calculations in Figures 5*a–l* in order to estimate the spectral type of DH Tau B, i.e., the effective temperature ( $T_{\text{eff}}$ ) and surface gravity ( $\log g$ ). We used the model spectra from the data provided by Tsuji et al. (2004) by tentatively assuming that DH Tau B is a dwarf ( $\log g = 5.5$ ), although the overall spectral shape has a strong dependence on  $\log g$  at  $T_{\text{eff}} < 2500$  K, which will be discussed later. We also employed the extinction of  $A_V = 0 - 4.4$  mag in order to accommodate the synthesized spectra to the observed near-infrared spectra and the optical fluxes measured on the *HST* archive data. Continuum veiling due to the circumstellar disk is assumed only in the  $K$ -band, with wavelength dependence as  $F_\lambda \propto \lambda^\alpha$  ( $\alpha > 0$ ). The observed spectra were fitted by a synthesized spectrum at each  $T_{\text{eff}}$  by minimizing the total residual at the three wavelength ranges of  $1.45 - 1.60 \mu\text{m}$ ,  $1.70 - 1.8 \mu\text{m}$  and  $2.0 - 2.45 \mu\text{m}$ .

Figures 5*a–l* show that the observed spectra are overall well fitted by a model spectrum either with  $T_{\text{eff}} = 1900$  K (Figure 5*d*) or  $2700 - 2800$  K (Figures 5*j* and *k*). Below  $1800$  K (Figures 5*a–c*), the calculated  $J$ -band fluxes are significantly smaller than the observed flux. The water absorption bands of the models become too deep for  $T_{\text{eff}}$  between  $2000$  K and  $2600$  K (Figure 5*e–i*), resulting in the excess  $H$ -band fluxes of model spectra. The  $J$ -band flux of the model again becomes too small at  $2900$  K.

In order to eliminate the temperature duality, we will use the equivalent width (EW) of the K I  $1.25 \mu\text{m}$  line. Although the overall shape of the observed spectra is fitted well in Figures 5*d*, *j* and *k*, the observed strength of the K I line is always smaller than those of the model spectra. We calculated from the data provided by Tsuji et al. (2004) the EW of K I as a function of  $T_{\text{eff}}$  with various realistic values of  $\log g$ . The results are presented in Figure 6*a*, showing that the EW

is always larger than the observed value for dwarfs ( $\log g = 5.5$ ) for  $T_{\text{eff}}$  lower than 2900 K. The observed EW is, however, accommodated with the smaller values of  $\log g = 4.0 - 5.0$  if  $T_{\text{eff}}$  is in the range between 2400 K and 2900 K. None of the realistic values of  $\log g$  can account for the EW if  $T_{\text{eff}}$  is less than 2200 K. We should therefore choose the higher  $T_{\text{eff}}$  solution for DH Tau B, but its surface gravity should be smaller than that of a dwarf. The smaller surface gravity does not significantly alter the overall shape of model spectra for the high  $T_{\text{eff}}$  solution as shown in Figure 7a, while it gives unacceptable change for the low  $T_{\text{eff}}$  solution as shown in Figure 7b. McGovern et al. (2004) also claimed that the weakness of KI lines is an indicative of low surface gravity for an object.

The EW of the Na I 2.21  $\mu\text{m}$  line may give further constraints. Figure 6b shows the dependence of its EW on  $T_{\text{eff}}$  and  $\log g$ , again calculated from the data provided by Tsuji et al. (2004). The EW of Na I increases with temperature especially when  $\log g$  is large. The observed EW is accommodated with any temperature between 2000 K and 3000 K if  $\log g = 3.5 - 4.5$ , while the model calculations predict significantly larger EWs if  $\log g \geq 5.0$  for  $T_{\text{eff}} > 2600$  K. We therefore conclude that DH Tau B has  $T_{\text{eff}} = 2700 - 2800$  K and  $\log g = 4.0 - 4.5$ . The same values are derived when we use the model of Allard et al. (2000).

Near-infrared spectra of low mass young stellar objects have often been compared to those of late type dwarfs ( $\log g = 5.5 - 6.0$ ). Our observations have shown, however, that overall spectral shapes, dominated by water absorption bands, are not sufficient to determine the spectral type and effective temperature of these objects, but the information of metallic lines is essential when the objects have smaller surface gravity. Gravity effects in young brown dwarfs is firstly analyzed by Lucas et al. (2001). An example of this is shown in Figure 8, where the observed spectra of DH Tau B ( $T_{\text{eff}} = 2700 - 2800$  K) are compared with that of Kelu 1 (L2,  $T_{\text{eff}} = 1900$  K, Leggett et al. 2001) and a model dwarf spectrum with  $T_{\text{eff}} = 1900$  K and  $\log g = 5.5$  taken from Tsuji et al. (2004). The spectra of DH Tau B are surprisingly similar to these low temperature dwarfs, except that it shows only a shallow K I absorption line.

### 3.3. DH Tau B as a Brown Dwarf Companion

The bolometric luminosity of DH Tau B is  $\sim 10^{-2.44} L_{\odot}$  derived from the synthesized spectra. From this luminosity together with the effective temperature, we estimated its mass and age of  $0.04 - 0.05 M_{\odot}$  and  $10^7$  yr, respectively, from the HR diagram of Baraffe et al. (2003) as shown in Figure 9a. If we use the result of D’Antona & Mazzitelli (1997), the mass and ages are  $0.03 - 0.04 M_{\odot}$  and  $3 \times 10^6 - 10^7$ , respectively (Figure 9b). DH Tau B is thus a brown dwarf companion to DH Tau A. The age of DH Tau B appears to be larger than that of  $10^5 - 4 \times 10^6$  yr of DH Tau A. Further discoveries of young brown dwarf companions, as well as precise measurement of the bolometric luminosity of DH Tau A will solve this mismatch in the age.

DH Tau A has another companion, DI Tau, with a separation of  $16''$ . Holman & Wiegert (1999)

investigated the stability of such multiple systems and concluded that a less massive tertiary has a stable orbit if its semi-major axis is less than about a quarter of the separation of the binary. DI Tau is thus located sufficiently far away to make the orbit of DH Tau B stable. The orbital period of DH Tau B is estimated to be  $\sim 6000$  yr and its orbital motion is  $0^{\circ}.06$  yr $^{-1}$  if we assume a pole-on geometry. This would cause a position angle change of DH Tau B with respect to A by  $0^{\circ}.30$  between the 1999 *HST* and 2004 Subaru/CIAO observations. The measured change of the position angle was  $0^{\circ}.47 \pm 0^{\circ}.12$  between the two epochs and may be within the consistent range.

Bonnell & Bastien (1992) and Bate (2000) proposed that companion brown dwarfs are formed through the gravitational collapse of a molecular cloud, discussing the deficiency of brown dwarf companions with small separations. Brown dwarf companions with wider separations like the case of DH Tau B are rather common according to this formation mechanism. Another possible mechanism of companion brown dwarf formation is the fragmentation of a circumstellar disk (Rice et al. 2003). Although this leads to the formation of a number of low-mass companions, most of them, especially less massive objects, escape from the system. The remaining objects have large semi-major axes ( $a > 500$  AU) and large eccentricities. The orbit determination of DH Tau B will then provide a clue for distinguishing the two mechanisms of companion brown dwarf formation.

#### 4. CONCLUSIONS

We have detected a young brown dwarf companion to the classical T Tauri star DH Tau using a coronagraphic camera CIAO on the Subaru Telescope. Their physical association was confirmed by the common proper motion that the primary and secondary shared.

(1) The companion brown dwarf has the *H*-band flux of 15 mag and is located at  $2''.3$  (330 AU) away from the primary.

(2) The near-infrared colors of the companion are consistent with those of young stellar objects. Its near-infrared spectra taken with CISCO on the Subaru Telescope show deep water absorption bands and strong K I and moderate Na I absorption lines, indicating its low temperature.

(3) Comparison of the observed companion spectra with model spectra gave its effective temperature and surface gravity of  $T_{\text{eff}} = 2700 - 2800$  K  $\log g = 4.0 - 4.5$ , respectively.

(4) We estimated the mass of  $30 - 50 M_{\text{Jupiter}}$  for the companion from published evolutionary tracks of low-mass objects.

We are grateful for constructive and useful comments from an anonymous referee. We also thank Kentaro Aoki and Sumiko Harasawa for their support for making observations. This work was supported by “The 21st Century COE Program: The Origin and Evolution of Planetary Systems” of the Ministry of Education, Culture, Sports, Science and Technology (MEXT). Y. I. is supported by the Sumitomo Foundation, the Ito Science Foundation, and a Grant-in-Aid for

Scientific Research No. 16740256 of the MEXT. The HST data presented in this paper was obtained from the Multimission Archive at the Space Telescope Science Institute (MAST). STScI is operated by the Association of Universities for Research in Astronomy, Inc., under NASA contract NAS5-26555. This work is conducted as a part of the Observatory Project of "Subaru Disk and Planet Searches".

## REFERENCES

- Allen, L. E., Myers, P. C., Di Francesco, J., Mathieu, R., Chen, H., Young, E. 2002, *ApJ*, 566, 993
- Baraffe, I. Chabrier, C., Barman, T.S., Allard, F., Hauschildt, P.H. 2003, *A&A*, 402, 701
- Bate, M.R. 2000, *MNRAS*, 314, 33
- Bessell, M., Brett, J. 1988, *PASP*, 100, 1134
- Bonnell, I., Bastien, P. 1992, *ApJ*, 401, 654
- Burrows, A., Marley, M., Hubbard, W.B. et al. 1997, *ApJ*, 491, 856
- Chauvin, G., Lagrange, A. M., Dumas, C., Zucherman, B., Mouillet, D., Song, I., Beuzit, J. L., Lowrance, P. 2004, *A&A*, 425, L29
- D'Antona, F., Mazzitelli, I. 1997, *Mem. Soc. Astron. Italiana*, 68, 807
- Dutrey, A., Guilloteau, S., Duvert, G., Prato, L., Simon, M., Schuster, K., Menard, F. 1996, *A&A*, 309, 493
- Gorlova, N.I., Meyer, M.R., Rieke, G.H., Liebert, J. 2003, *ApJ*, 593, 1074
- McGovern, M. R., Kirkpatrick, J. D., McLean, I. S., Burgasser, A. J., Prato, L., Lowrance, P. J. 2004, *ApJ*, 600, 1020
- Hanson, R.B., Klemola, A.R., Jones, B.F., Monet, D.G. 2003, *Lick NPM2 Catalog*
- Hartigan, P., Strom, K.M., Strom, S.E. 1994, *ApJ*, 427, 961
- Hayashi, C., Nakano, T., 1963, *Prog. Theor. Phys.*, 30, 460
- Holman, M.J., Wiegert, P.A. 1999, *AJ*, 117, 621
- Holtzman, J. A., Hester, J. J., Casertano, S. et al. 1995, *PASP*, 107, 156
- Itoh, Y., Tamura, M., Gatley, I. 1996, *ApJ*, 465, L129
- Itoh, Y., Tamura, M., Takami, H., Takato, N. 1998, *PASJ*, 50, 55
- Itoh, Y., Tamura, M., Hayashi, S. S., et al. 2002, *PASJ*, 54, 963
- Jones, B.F., Herbig, G.H 1979, *AJ*, 84, 1872
- Kitamura, Y., Momose, M., Yokogawa, S., Kawabe, R., Tamura, M., Ida, S. 2002, *ApJ*, 581, 357
- Koornneef, J. 1983, *A&A*, 128, 84
- Leggett, S.K., Allard, F., Geballe, T.R., Hauschildt, P.H., Schweitzer, A. 2001, *ApJ*, 548, 908

- Leggett, S.K., Golimowski, D.A., Fan, X. et al. 2002, *ApJ*, 564, 452
- Lowrance, P.J., McCarthy, C., Becklin, E.E., et al. 1999, *ApJ*, 512, L69
- Lowrance, P.J., Schneider, G., Kirkpatrick, et al. 2000, *ApJ*, 541, 390
- Lucas, P. W., Roche, P. F., Allard, F., Hauschildt, P. H. 2001, *MNRAS*, 326, 695
- Luhman, K. L., Stauffer, J. R., Muench, A. A., Rieke, G. H., Lada, E. A., Bouvier, J., Lada, C. J. 2003, *ApJ*, 593, 1093
- Mainzer, A. K., McLean, I. S. 2003, *ApJ*, 597, 555
- Meyer, M. R., Beckwith, S. V. W., Herbst, T. M., Robberto, M. 1997a, *ApJ*, 489, L173
- Meyer, M. R., Calvet, N. A., Hillenbrand, L. A. 1997b, *AJ*, 114, 288
- Monet, D.G., Levine, S.E., Casian, B., et al. 2003, *AJ*, 125, 984
- Nakajima, T., Oppenheimer, B.R., Kulkarni, S.R., et al. 1995, *Nature*378, 463
- Oasa, Y., Tamura, M., Sugitani, K. 1999, *ApJ*, 456, 292
- Oppenheimer, B.R., Kulkarni, S.R., Matthews, K., van Kerkwijk, M.H. 1995, *Science*, 270, 1478
- Reipurth, B., Clarke, C. 2001, *AJ*, 122, 432
- Rice, W.K.M., Armitage, P.J., Bonnell, I.A., Bate, M.R., Jeffers, S.V., Vine, S.G. 2003, *MNRAS*, 346, L36
- Simon, M., Close, L. M., Beck, T. L. 1999, *AJ*, 117, 1375
- Strom, K.M., Strom, S.E., Edwards, S., Cabrit, S., Strutskie, M.F. 1989, *AJ*, 97, 1451
- Tamura, M., Sato, S. 1989, *AJ*98, 1368
- Tamura, M., Suto, H., Itoh, Y., Ebizuka, N., Doi, Y., Murakawa, K., Hayashi, S. S., Oasa, Y., Takami, H., Kaifu, N. 2000, *Proc. SPIE*, 4008, 1153
- Tsuji, T., Nakajima, T., Yanagisawa, K. 2004, *ApJ*607, 511
- White, R.J., Ghez, A.M., Reid, I.N., Schultz, G. 1999, *ApJ*, 520, 811
- White, R.J., Ghez, A.M. 2001, *ApJ*, 556, 265
- Zacharias, N., Urban, S.E., Zacharias, M.I., Wycoff, G.L., Hall, D.M., Monet, D.G., Rafferty, T.J. 2004, *AJ*, 127, 3043
- Zapatero-Osorio, M. R., Béjar, V. J. S., Martín, E. L., Rebolo, R., Barrado y Navascués, D., Mundt, R., Eisloffel, J., Caballero, J. A. 2002, *ApJ*, 578, 536

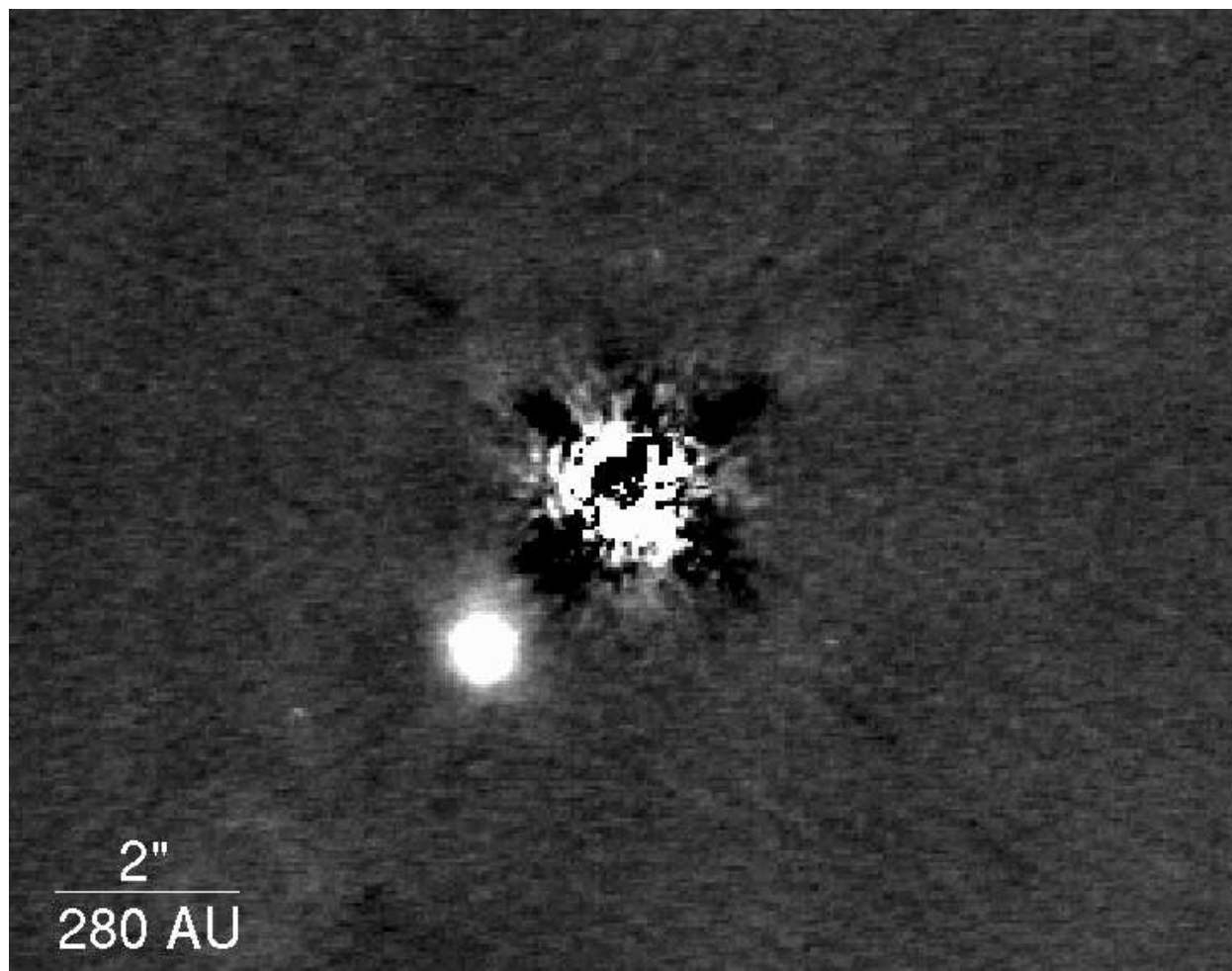


Fig. 1.— *K*-band coronagraphic image of DH Tau. North is up and east is to the left. The primary star (DH Tau A) is located at the center of the image but is blocked by the mask. The companion (DH Tau B) is detected at  $\sim 2''.34$  south-east of DH Tau A.

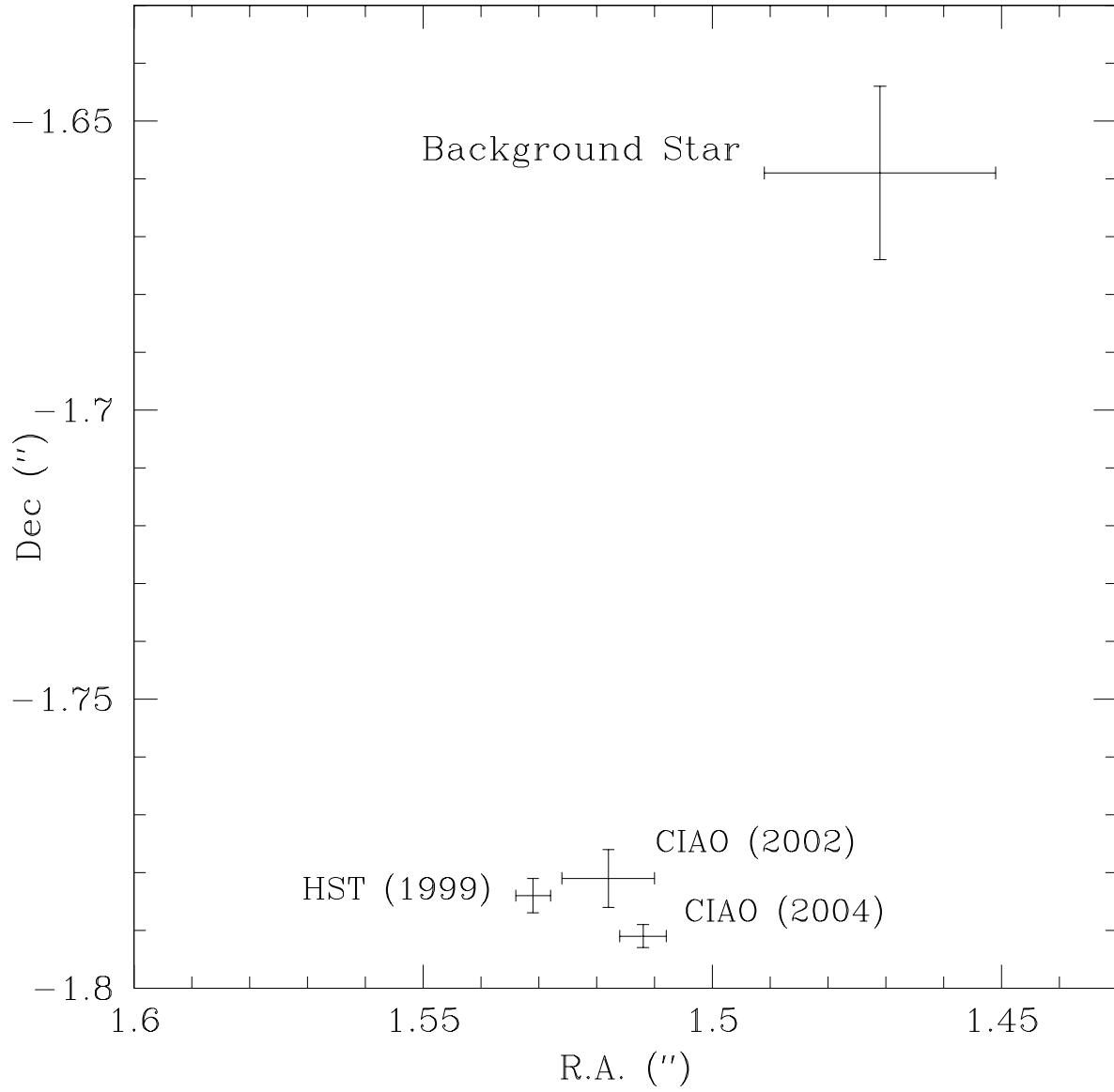


Fig. 2.— Astrometric measurements of DH Tau B. Offset positions are shown with respect to DH Tau A. The expected position of a distant background star on 2004 January is shown by assuming that it was located at the *HST* position on 1999 January.

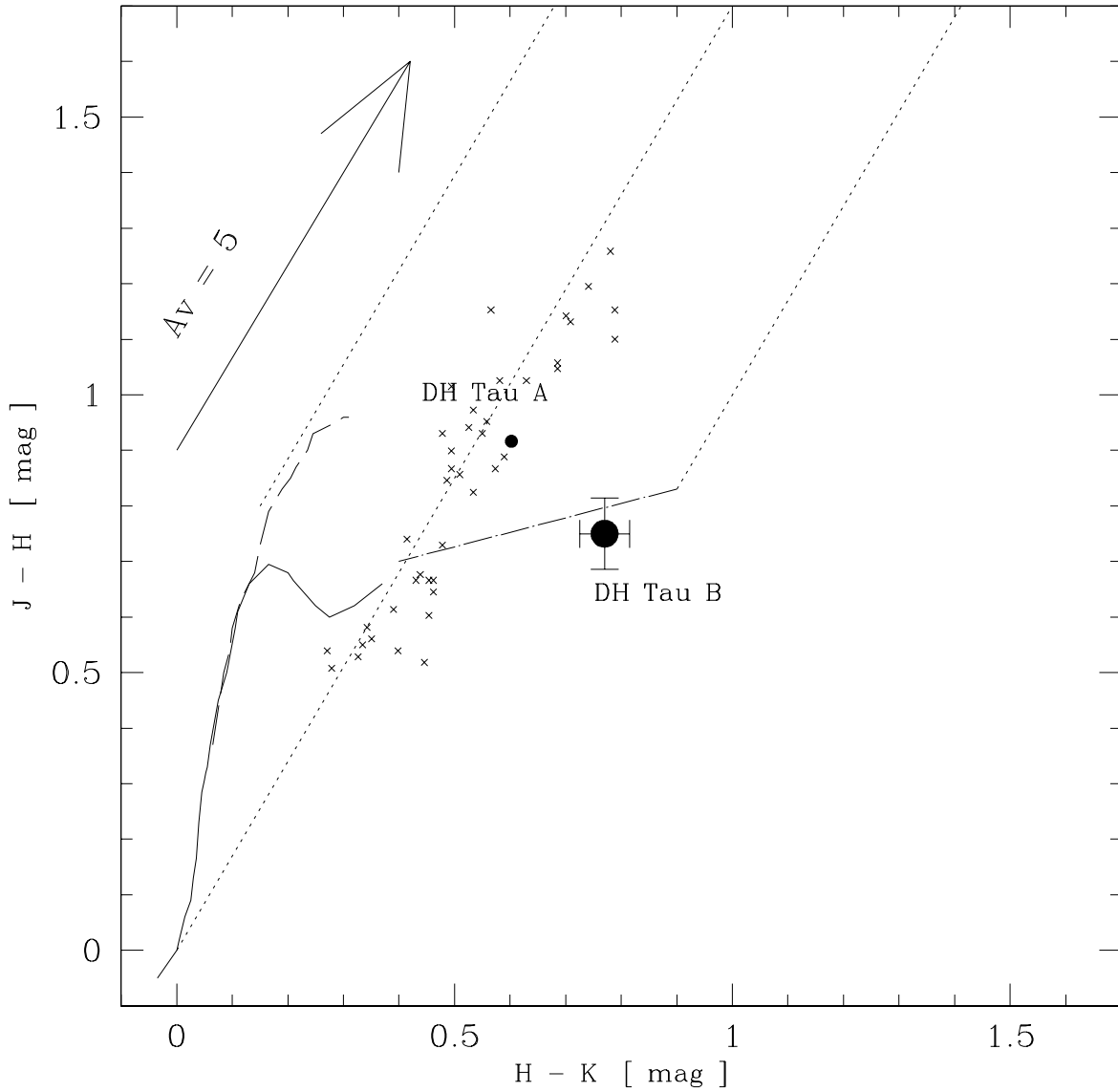


Fig. 3.— The near-infrared colors of DH Tau A and B. Also plotted are the near-infrared colors of main-sequence stars (solid line; Bessell & Brett 1988), giants (dashed line; Koornneef 1983), classical T Tauri stars (dot-dashed line; Meyer et al. 1997b), and L-type brown dwarfs (crosses; Leggett et al. 2002). All colors are transformed into the CIT system.

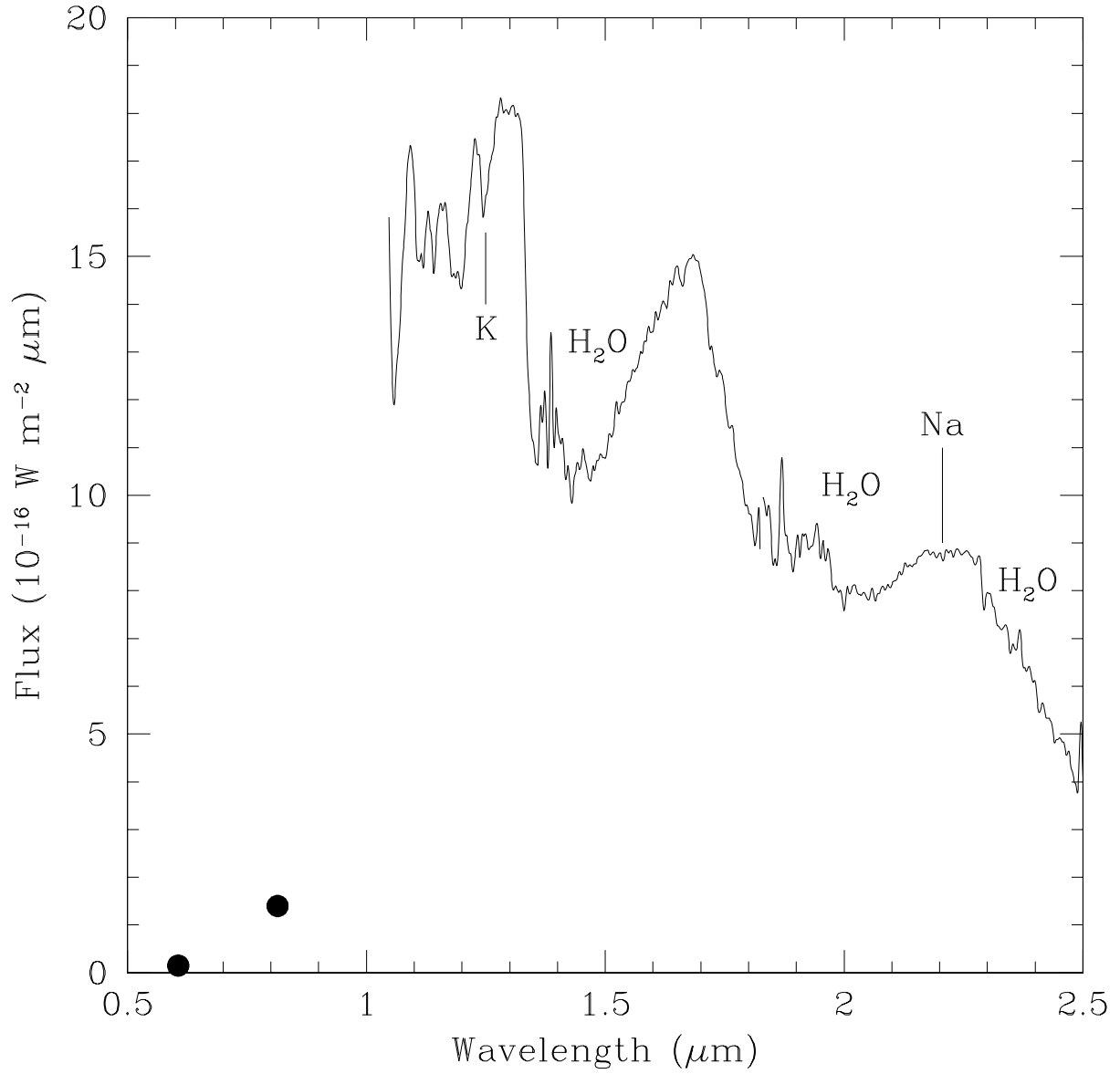


Fig. 4.— The near-infrared spectra of DH Tau B. Optical broad-band fluxes were measured on the *HST* archive data.

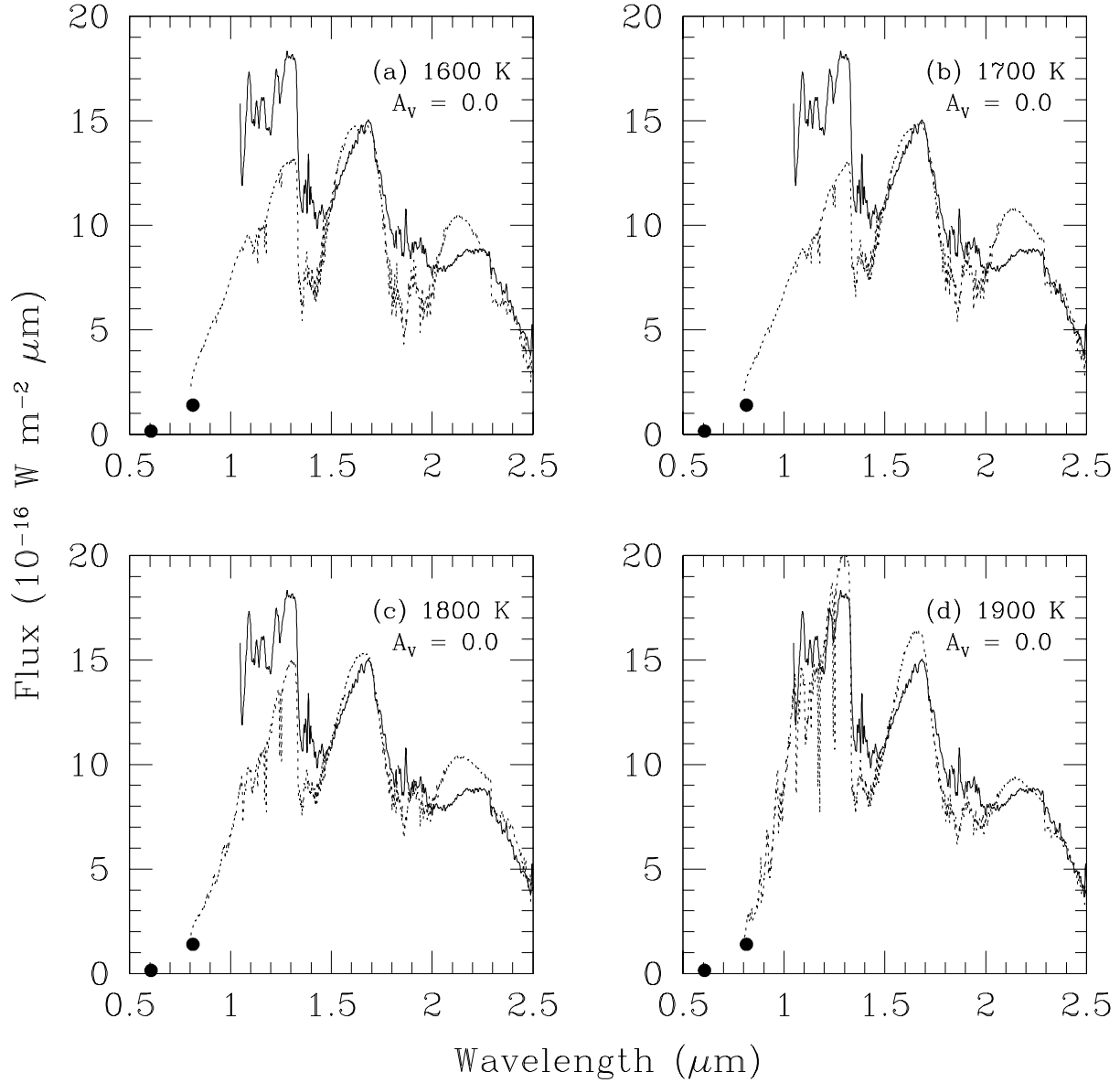
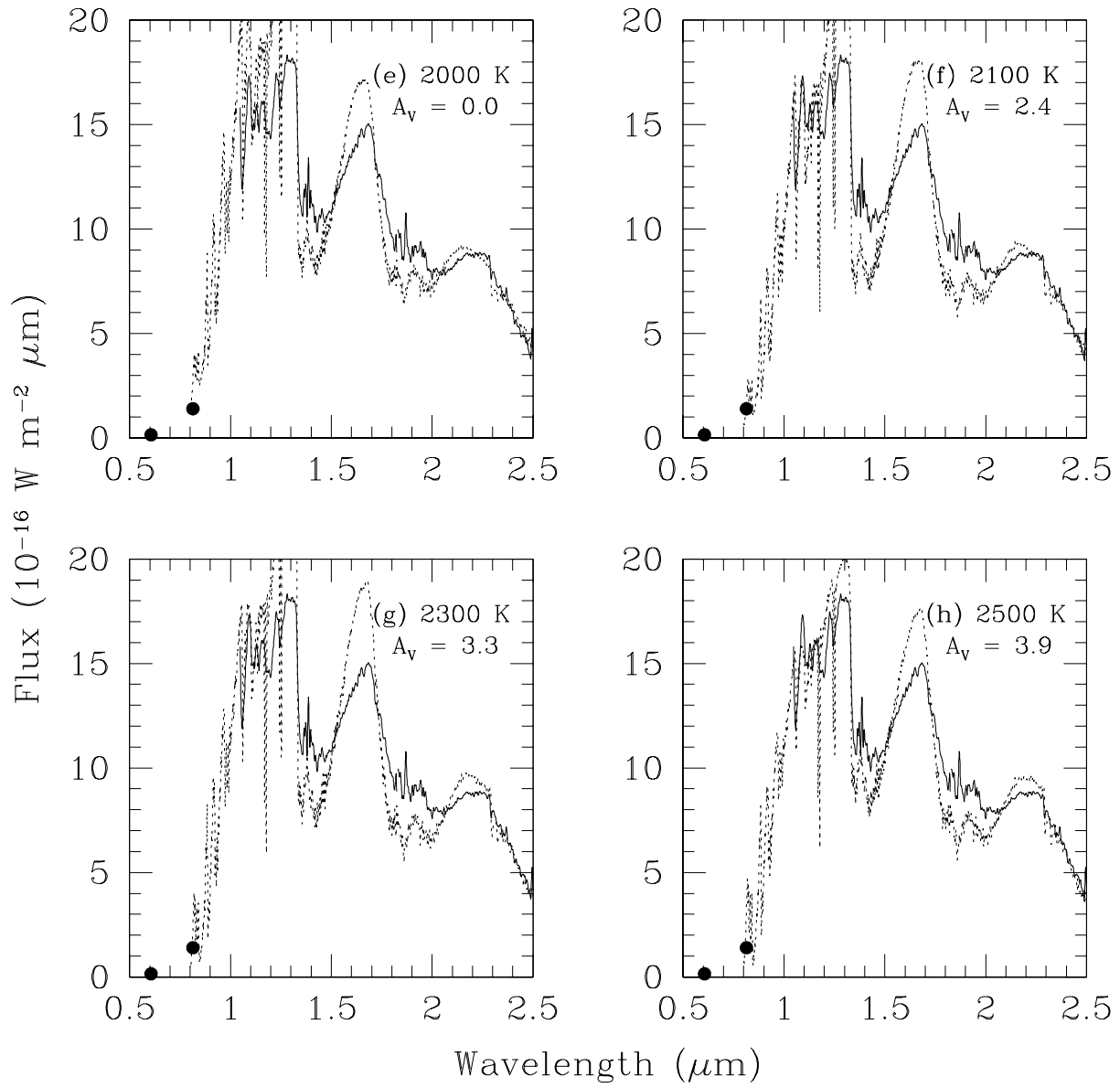
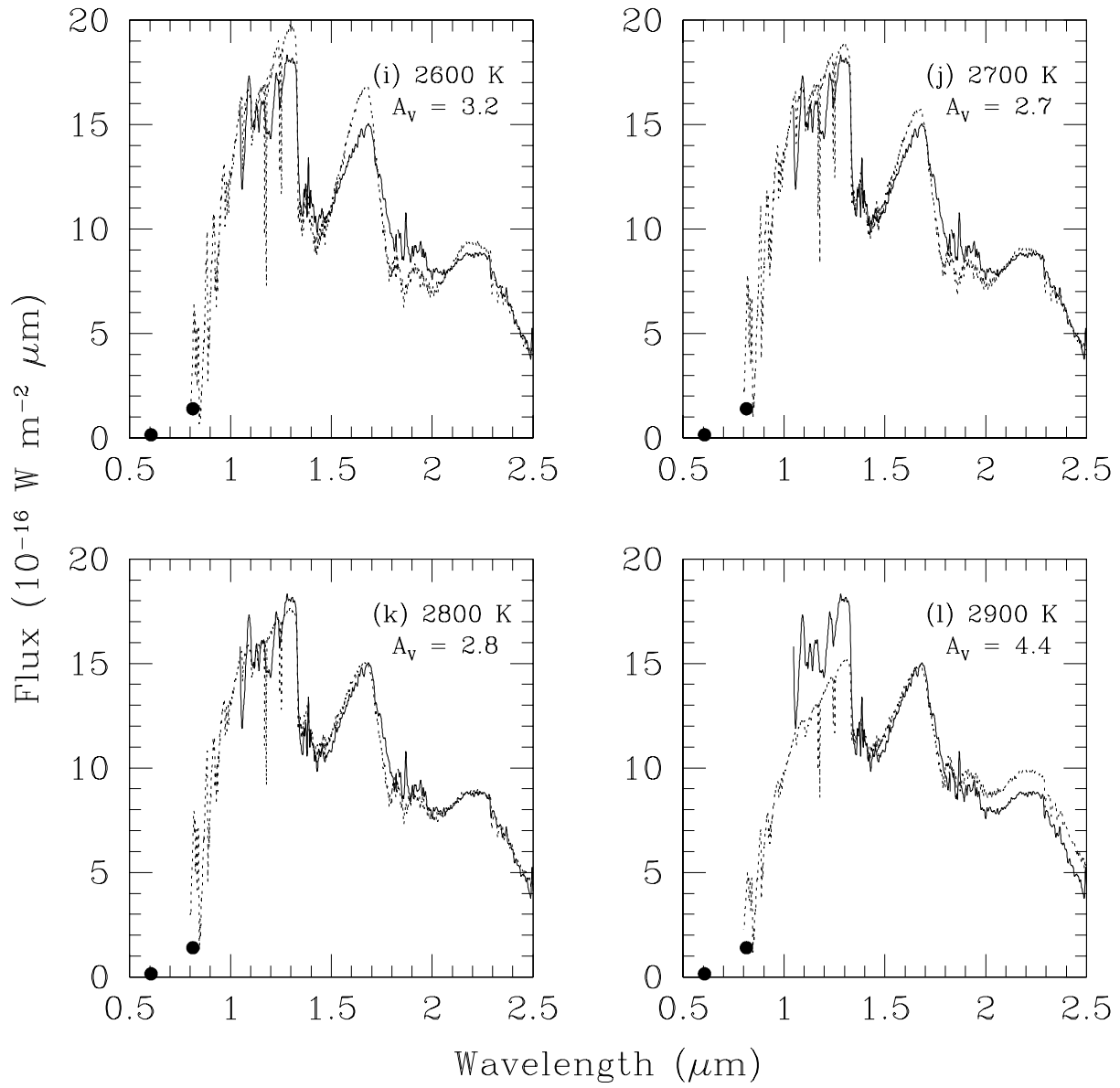


Fig. 5.— The near-infrared spectra of DH Tau B (solid line) are shown in each panel together with the best fit synthesized spectrum with  $\log g = 5.5$  (dotted line) for the effective temperature ranging from 1600 K to 2900 K. The assumed visual extinction is also shown in each panel.





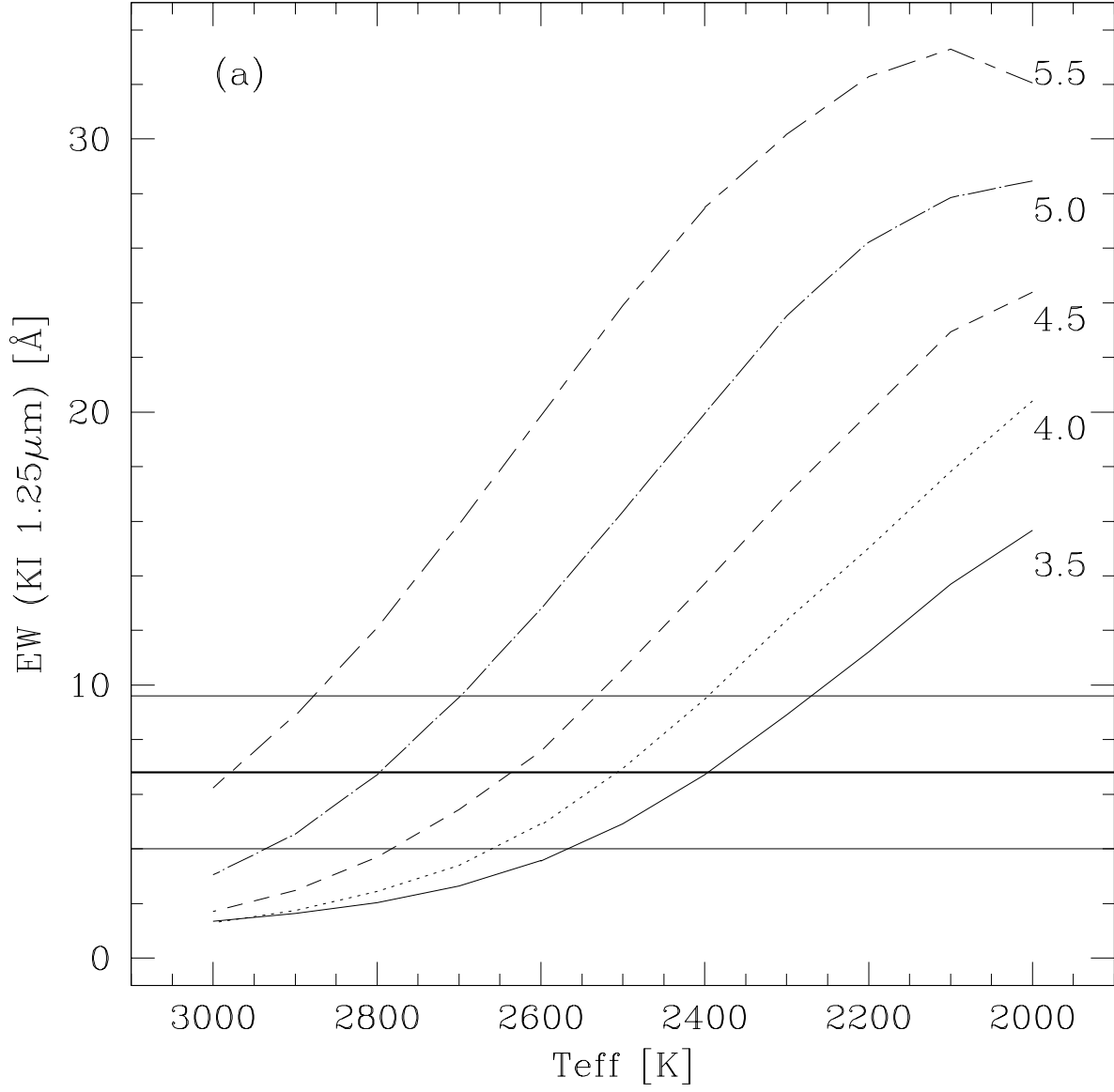
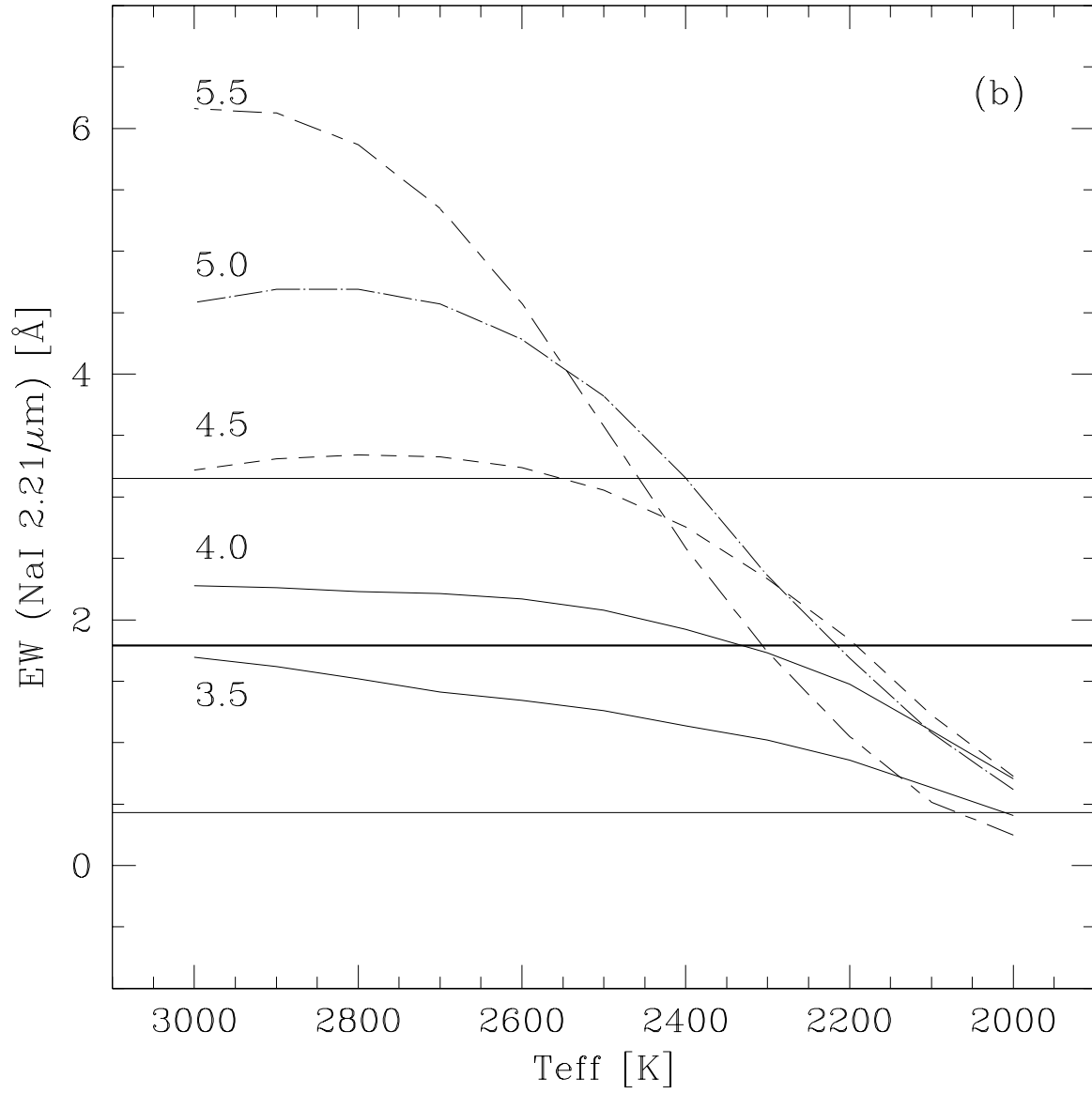


Fig. 6.— (a) The equivalent width of the K I line is shown as a function of the effective temperature with each curve representing a different value of the surface gravity  $\log g$  given in its right. The thick and thin lines are the observed equivalent width and its error. (b) Same as (a) but for the Na I line.



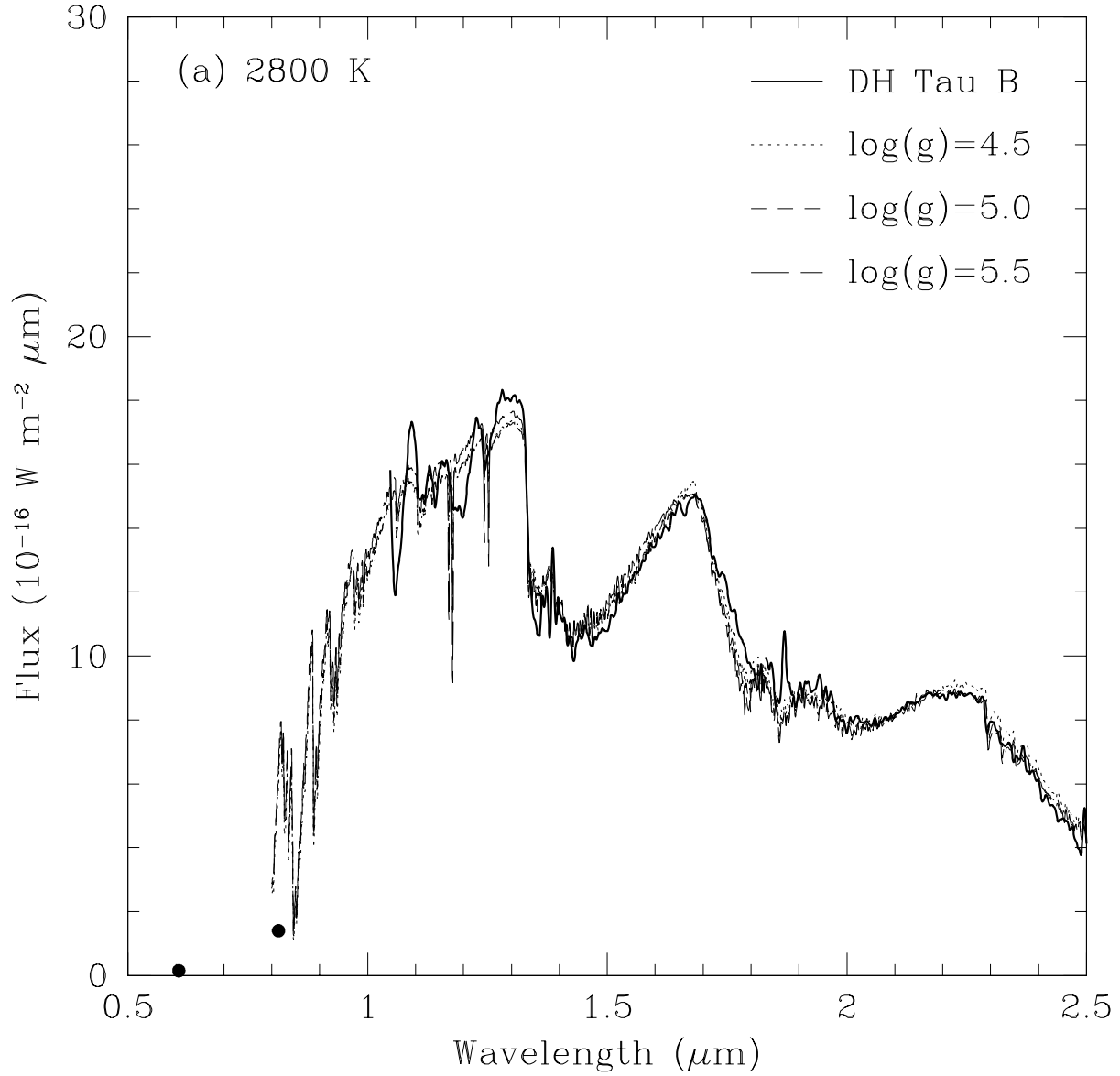
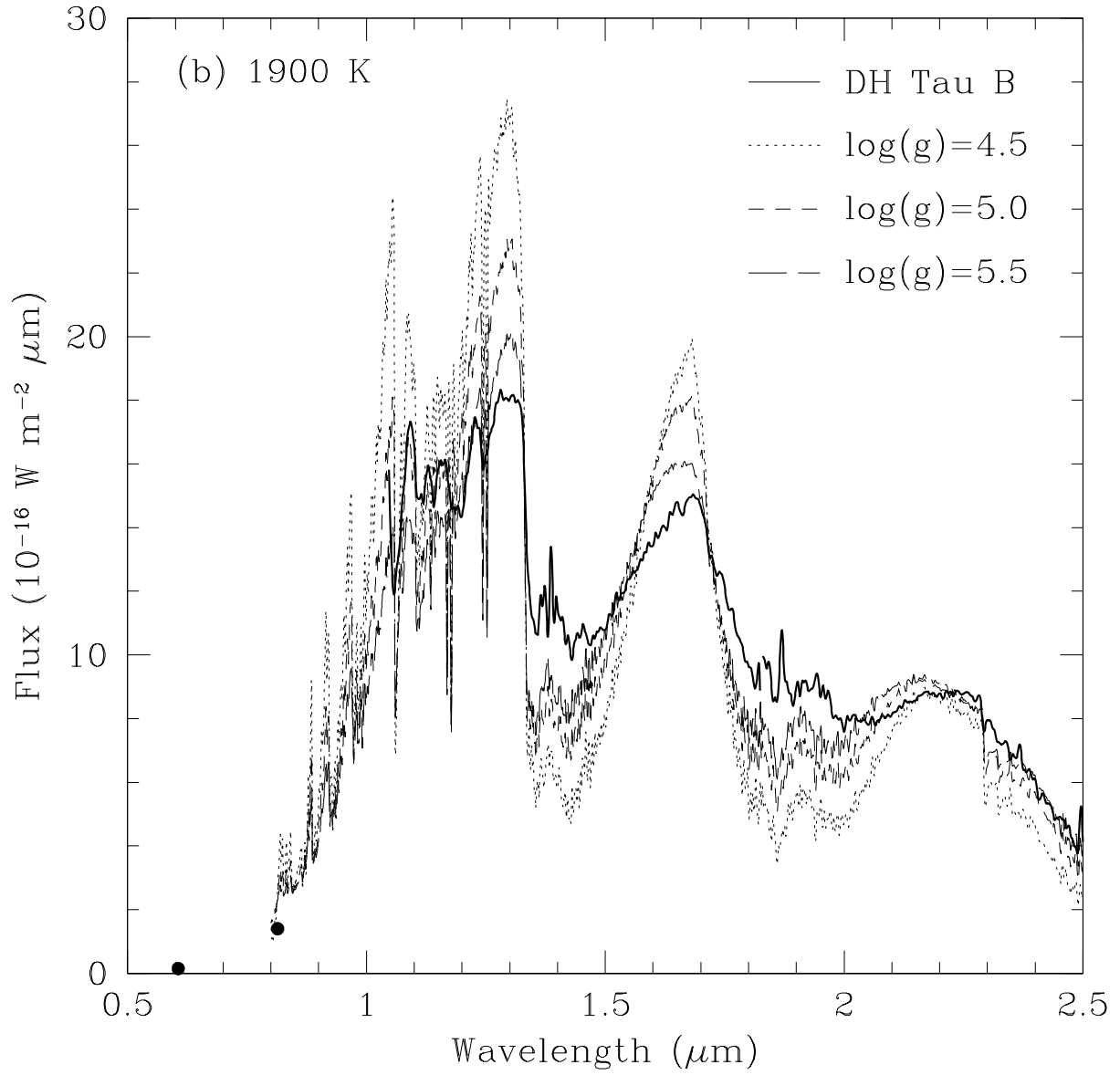


Fig. 7.— (a) The near-infrared spectra of DH Tau B are compared with the synthesized spectra with three different values of the surface gravity for  $T_{\text{eff}} = 2800 \text{ K}$ . (b) Same as (a) but for  $T_{\text{eff}} = 1900 \text{ K}$ .



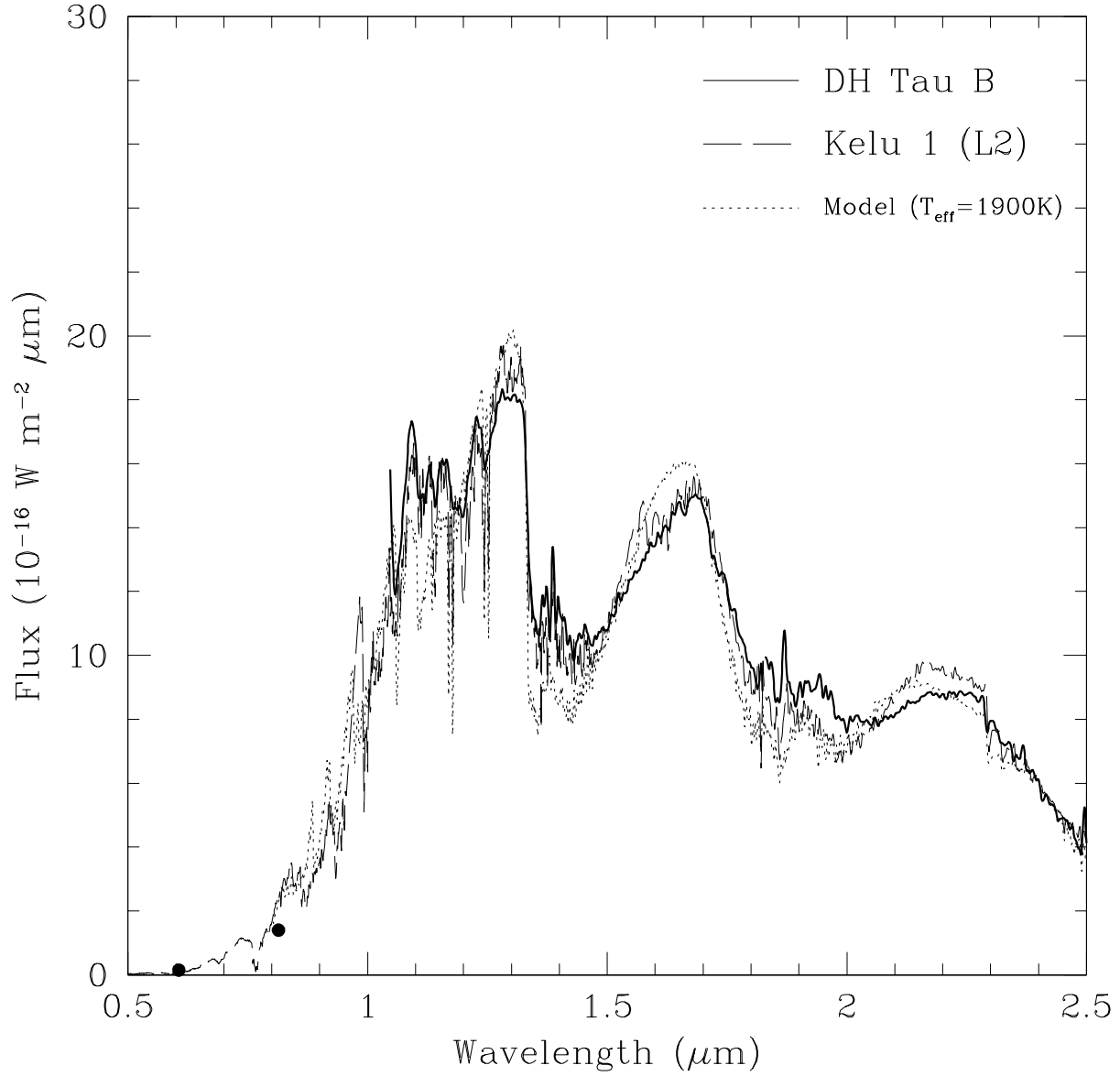


Fig. 8.— The near-infrared spectra of DH Tau B are compared with that of the L2 dwarf Kelu 1 (Leggett et al. 2001) and a synthesized spectrum of  $T_{\text{eff}} = 1900 \text{ K}$  and  $\log(g) = 5.5$ .

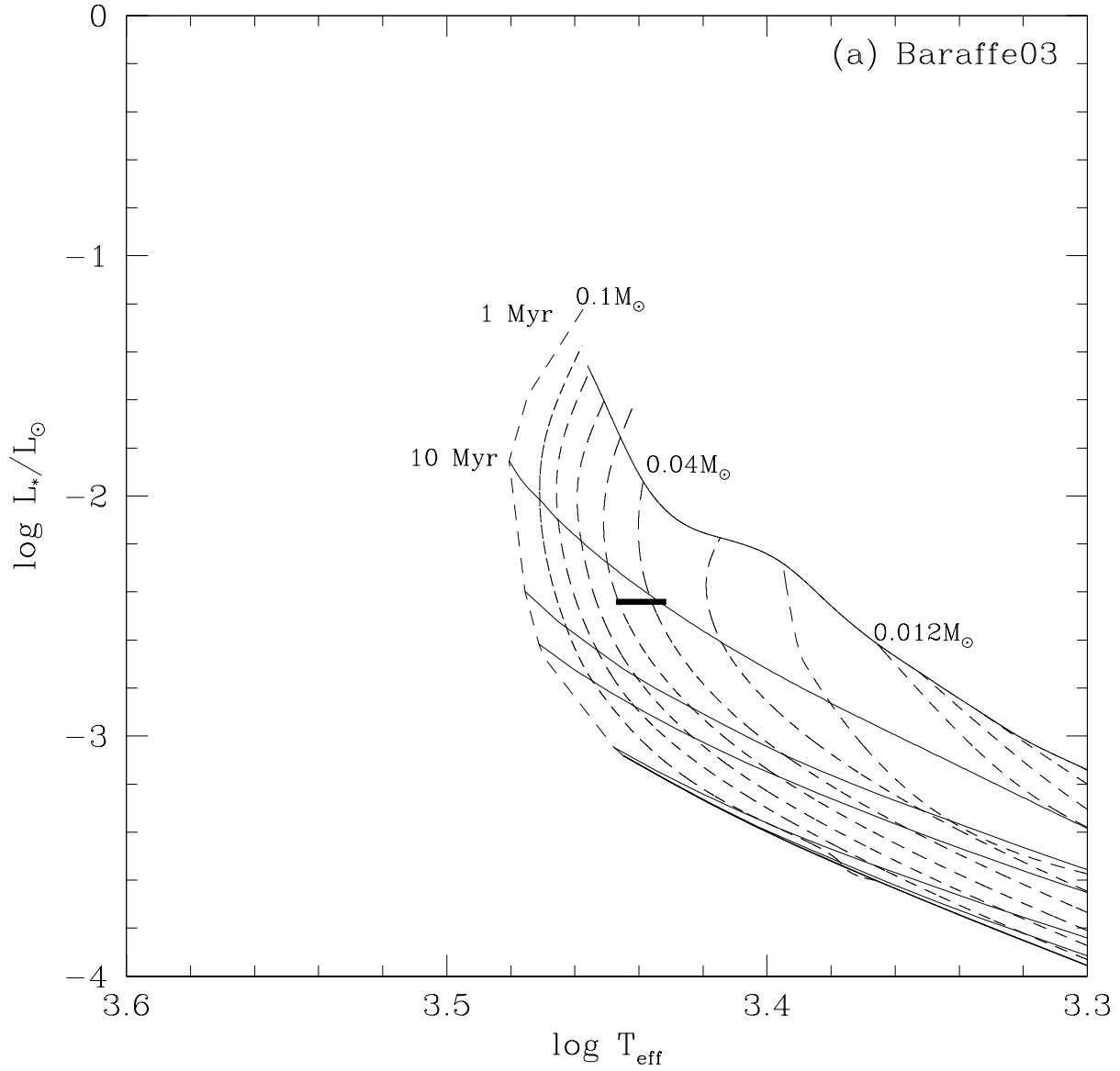


Fig. 9.— (a) The location of DH Tau B on the evolutionary tracks of Baraffe et al. (2003). (b) same as (a) but on the evolutionary tracks of D’Antona & Mazzitelli (1997). "H", "M", and "W" are the positions of DH Tau A (Hartigan et al. 1994; Meyer et al. 1997a; White & Ghez 2001).

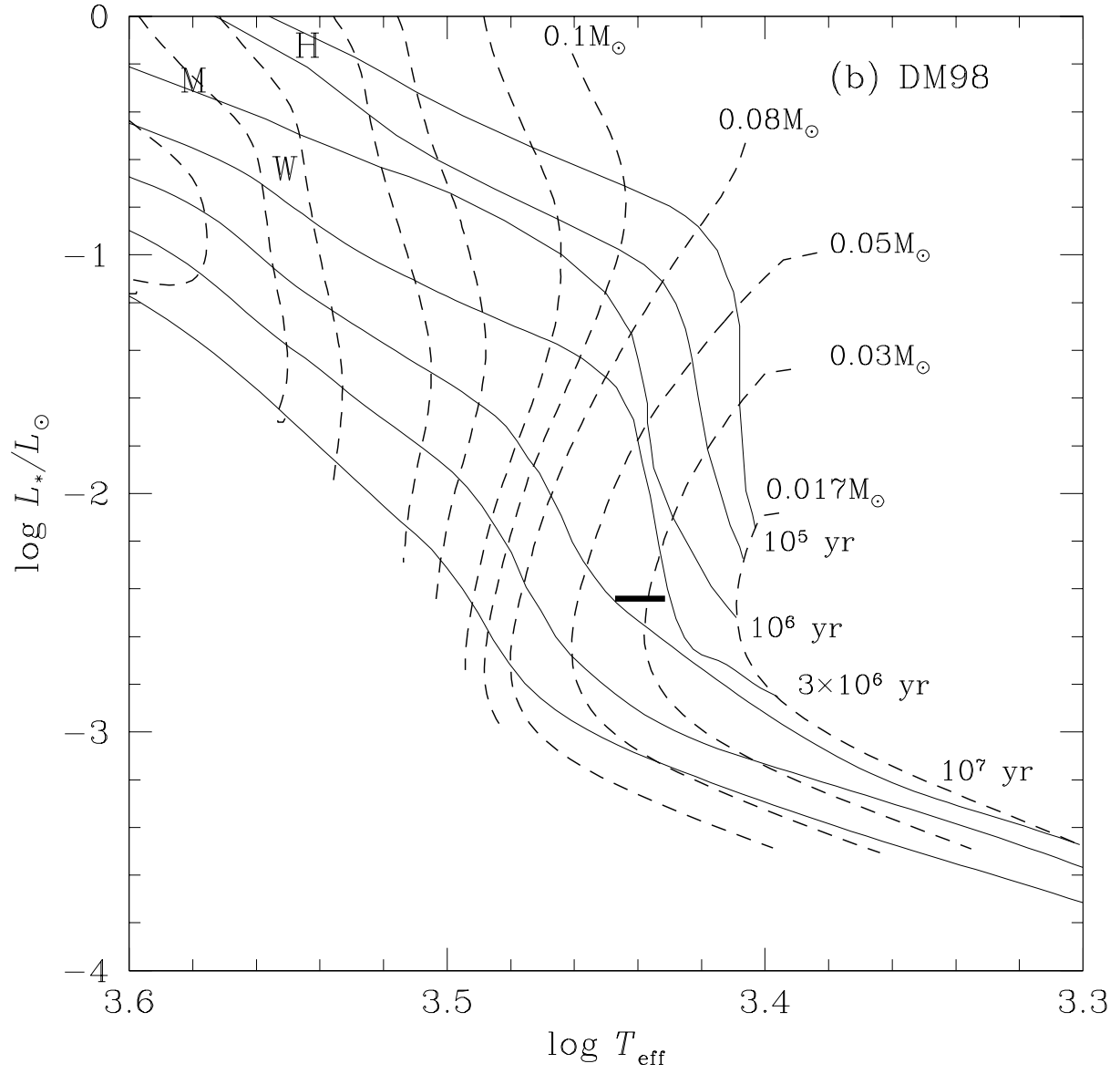


Table 1: Observation log.

date	band	exposure	total integ. time
Coronagraphy			
2002 Nov. 23	<i>H</i>	10 sec×3 coadd×24 frames	720 sec
2004 Jan. 8	<i>J</i>	10 sec×3 coadd×24 frames	720 sec
	<i>H</i>	10 sec×3 coadd×24 frames	720 sec
	<i>K</i>	10 sec×3 coadd×24 frames	720 sec
Spectroscopy			
2003 Nov. 8	<i>K</i>	300 sec×1 coadd×4 frames	1200 sec
2004 Jan. 9	<i>JH</i>	300 sec×1 coadd×12 frames	3600 sec